SAN097-0152C

INTERFACIAL ARSENIC FROM WET OXIDATION OF $Al_xGa_{1-x}As$/GaAs: ITS EFFECTS ON ELECTRONIC PROPERTIES AND NEW APPROACHES TO MIS DEVICE FABRICATION

CONF-961202--21 SAND--97-0152C

CAROL I.H. ASHBY, JOHN P. SULLIVAN, PAULA P. NEWCOMER, NANCY A. MISSERT, HONG Q. HOU, B.E. HAMMONS, MICHAEL J. HAFICH, ALBERT G. BACA
Sandia National Laboratories, P.O. Box 5800, Albuquerque, NM 87185-0603

ABSTRACT

Three important oxidation regimes have been identified in the temporal evolution of the wet thermal oxidation of $Al_xGa_{1-x}As$ ($1 \geq x \geq 0.90$) on GaAs: 1) oxidation of Al and Ga in the $Al_xGa_{1-x}As$ alloy to form an amorphous oxide layer, 2) oxidative formation and elimination of elemental As (both crystalline and amorphous) and of amorphous As_2O_3, and 3) crystallization of the oxide film. Residual As can result in up to a 100-fold increase in leakage current and a 30% increase in the dielectric constant and produce strong Fermi-level pinning and high leakage currents at the oxidized $Al_xGa_{1-x}As$/GaAs interface. The presence of thermodynamically-favored interfacial As may impose a fundamental limitation on the application of AlGaAs wet oxidation for achieving MIS devices in the GaAs material system.

INTRODUCTION

There is a continuing quest to find a good insulator for metal-insulator-semiconductor (MIS) devices to enable the GaAs-equivalent of Si CMOS technology. Earlier approaches involving dry thermal oxides and anodic oxides have not yielded interfaces of sufficient quality (interface-state densities in the mid-10^{10} /cm^2-eV) for MIS applications. A relatively new approach to forming a technologically useful oxide involving oxidation of high-Al-content AlGaAs layers at elevated temperature during exposure to wet nitrogen [1] has shown promise for forming readily manufacturable stable oxides that might prove suitable for MIS applications [2]. We have studied the temporal evolution of AlGaAs films undergoing wet oxidation using Raman spectroscopy to identify product species that are present during the intermediate and final stages of the oxidation and have determined electrical properties of the Al-oxide/GaAs materials system using DC transport and capacitance measurements. These studies reveal a fundamental limitation on the application of AlGaAs wet oxidation for achieving MIS devices in the GaAs material system.

EXPERIMENT

Samples with the following structure were grown by MOCVD: 300 Å GaAs cap/ variable thickness $Al_xGa_{1-x}As$/1000 Å GaAs/GaAs substrate with x= 1.0, 0.98, and 0.90. Raman studies employed 0.25- and 2-μm $Al_xGa_{1-x}As$ layers, while diffraction (X-ray and electron) and bulk electrical measurements were performed on 0.25-μm $Al_xGa_{1-x}As$ samples. MIS diode samples consisted of 300-500 Å of $Al_xGa_{1-x}As$ on 2-5x10^{16}/cm^3 n-GaAs.

Prior to wet oxidation , the GaAs cap was removed by a selective etch in a citric acid/peroxide mix (5:1 of [1g citric monohydrate/1g H_2O]:30% H_2O_2) and the sample was loaded into the furnace under a dry nitrogen purge. The sample was then heated under flowing nitrogen. When the desired reaction temperature was reached (400<T<455 °C), the nitrogen flow (typically 0.4 slm in a 2-in. diam. tube) was switched to bubble through water at a temperature of 80° ± 1

DISCLAIMER

for a timed reaction. Dry nitrogen flow was restored at the completion of the reaction time and continued during sample removal from the furnace.

Raman spectra were measured using an excitation wavelength of 514.5 nm. The 500-mW probe beam was line focused to apply less than 85 W/cm^2 on the sample. Scattering was measured in the $x(y',y'+z')\bar{x}$ backscattering configuration with y' and z' parallel to (110) planes. A triple monochromator with an internal depolarizer and a CCD array detector were employed. Reference Raman spectra were obtained for α-Al_2O_3 (99.997%, 110 μm crystalline, 9 m^2/g surface area) and γ-Al_2O_3 (99.999%, 110 μm powder, 55 m^2/g surface area). Peak positions in cm^{-1} and relative intensities for α-Al_2O_3 were as follows: 379 (0.34), 417(1), 428(0.28), 458(0.06), 576(0.11), 644(0.24), 750(0.23). X-ray measurements on γ-Al_2O_3 showed a broad amorphous background with broad peaks; using the Scherrer formula gives a crystallite size of 70 Å. Weak Raman peaks from γ-Al_2O_3 were observed at 385, 468, 624, 644, 750 cm^{-1}. This small crystallite size might cause red-shifting and asymmetric broadening of the peaks [3]; low signal intensity prevented evaluation of this possible effect.

X-ray diffraction measurements were performed on the films using Cu K-alpha radiation from a fixed anode source and a curved graphite crystal detector. Conventional Θ-2Θ scans were taken between 10° and 70°, corresponding to lattice spacings of 8.8 Å-1.34 Å. Cross-section samples for high resolution transmission electron microscopy were prepared by mechanical thinning and ion milling with 5 kV Ar^+ and examined at 200 keV using a JEOL 2010 at the University of New Mexico. Samples for electrical characterization were prepared by shadow mask deposition of Ti/Au circular contacts (200-1000 μm) on the oxide surface followed by deposition of a non-alloyed ohmic backside contact. For bulk dielectric measurements, 0.25 μm thick oxidized $Al_xGa_{1-x}As$ layers on top of near-degenerately n-doped GaAs were used in order to minimize the interfacial depletion layer capacitance. For interface electrical characterization, thinner $Al_xGa_{1-x}As$ layers were measured on 2-5x10^{16} cm^{-3} n-doped GaAs buffer layers. Capacitance-voltage measurements (Fig. 2) were performed over the frequency range 100 kHz to 1 MHz, typically 1 MHz, at a sweep rate of 150 mV/min. DC transport measurements were performed over the range -5 V to 5 V under dark conditions.

RESULTS AND DISCUSSION

Progressive oxidation of the AlGaAs layer reduces the phonon peak intensity at 400 cm^{-1}, as shown in Fig. 1 for 2-μm AlGaAs samples. Substrate GaAs is manifest at 292 cm^{-1} due to the low absorption coefficient of indirect-gap $Al_{0.98}Ga_{0.02}As$ at 514.5 nm. The Raman spectrum of a partially oxidized film is dominated by crystalline As° peaks at 198 and 257 cm^{-1} and broad feature between 200 and 250 cm^{-1} peaking near 227 cm^{-1} ascribed to amorphous As° [4]. The As° peaks are very strong due to resonant enhancement of the Raman scattering at this excitation energy; the detection limit is on the order of 10-20-Å layers [5]. The broad feature centered at 475 cm^{-1} is due to amorphous As_2O_3 [5]. Specific peaks associated with amorphous Al-oxides are not observed. Gallium oxide films of 8000-Å thickness are not detectable by Raman because of low cross section [5], and the less polarizable Al-oxide films should be even weaker scatterers. Since the relative intensities of the various peaks cannot be construed as a quantitative measure of the different compositions due to large and quantitatively unknown differences in their scattering cross sections, the following discussion is qualitative.

As the oxidation front advances into films of either AlAs or high-Al-fraction AlGaAs, there is established a relatively constant Raman signal from As and a-As_2O_3 while the intensity of the AlAs-like phonon decreases (Fig 1a-c.) Growth of the amorphous Al-oxide film is manifested by

the gradually rising baseline. As oxidation of the $Al_xGa_{1-x}As$ layer nears completion, the AlAs-like phonon peak drops below our detection limit. The a-As_2O_3 peak intensity also drops below the detection limit. There remains barely detectable scattering from As near the oxide/GaAs interface and a steeply rising baseline (Fig. 1d). With continued exposure to the oxidizing atmosphere or with annealing in vacuum or dry nitrogen, crystallization of the films occurs (Fig. 1e), with most of the strong peaks attributable to Rayleigh scattering of laser plasma or background light or to GaAs-associated features typically observed on rough GaAs, where polarization selection rules that are operative with specular surfaces break down. Weak peaks at 750 and 644 cm^{-1} ascribed to γ-Al_2O_3 are observed in crystallized films. Delamination of the 2.0-μm films routinely occurs after complete oxidation, suggesting relatively weak adhesion between the oxide and semiconductor. This is consistent with the relative fragility of laterally oxidized optoelectronic structures when subjected to cleaving operations.

We propose the following reaction scenario for Al(Ga)As films undergoing wet oxidation. Al(Ga)As undergoes reaction with water, hydroxyl, or other oxygen-containing species derived from water to form a mixture of aluminum(gallium) oxides and/or hydroxides and amorphous As_2O_3, which forms a glassy matrix and prevents wide-scale crystallization. Elemental As (As^0) is present at the interface between the oxide and the semiconductor, and a relatively constant amount is observed throughout most of the oxidation. This amount is determined by the kinetic balance between its formation and subsequent loss through further oxidation or volatilization and escape through the permeable oxide film; this balance will vary with specific reaction conditions. TEM studies of laterally wet-oxidized AlGaAs layers have shown the oxide layer to be far from fully dense and should have adequate permeability for ready escape of volatile reaction products [6]. Both As (P(vap) = 760 Torr at 407 °C) and a- As_2O_3 (P(vap) = 760 Torr at 320 °C) may serve as volatile products for removal of As from the growing oxide film. It has been postulated that arsine is the major product of AlGaAs wet oxidation. We cannot rigorously exclude a role for arsine as a minor product, since our furnace was not equipped for identification of volatile products. However, our observation of two volatile As-species in more highly oxidized states than the original AlGaAs suggests that formation of major quantities of the lower oxidation state arsine as the volatile reaction product is unnecessary for As removal from the oxidized film.

Figure3 shows high-resolution transmission electron micrographs (TEM) of the interfacial region between GaAs and $Al_{0.90}Ga_{0.10}As$ as the reaction approaches completion. Moiré fringes due to a 2-4 nm crystallite at the interface and lattice fringes associated with unreacted $Al_{0.90}Ga_{0.10}As$ are observed near the oxide/GaAs interface. Selected area diffraction taken within the oxidized $Al_{0.90}Ga_{0.10}As$ layer show diffuse polycrystalline rings with d-spacings corresponding to the prominent reflections of γ-Al_2O_3. X-ray diffraction measurements on similar films reveal only a diffuse background with no apparent crystalline Al_2O_3 phases, thus putting an upper limit on crystallite size of ~ 10 nm. The lower magnification image of Fig. 3 reveals that the interfaces are not abrupt, but exhibit interfacial roughness on the order of 2-4 nm.

The temporal evolution of the structure of these surface-oxidized films correlates with that observed along the length of a laterally-oxidized buried layer[6]. At the oxide/semiconductor interface of a laterally oxidized layer, an amorphous meniscus is observed. Farther back from the oxidation front the oxidized layer consists of increasingly crystalline gamma γ- Al_2O_3.. Since increasing distance from the oxidation front in a laterally oxidized sample correlates with increasing oxidation time, the evolution from amorphous to crystalline structures in both laterally and surface-oxidized samples is probably do to progressive loss of the stabilizing glassy matrix provided by a-As_2O_3.

The results of capacitance and DC transport measurements on 0.25-μm wet-oxidized films as a function of residual As and Ga content are shown in Table 1. Samples labeled as "high"

arsenic exhibit As^0 Raman signals on the order of those shown in Fig. 1 while "low" arsenic samples exhibit As^0 signals below the Raman detection limit. Residual As^0 can result in up to a two order of magnitude increase in leakage current and up to a 30% increase in the dielectric constant. The increase in dielectric constant with increasing As concentration may be partly due to dielectric heterogeneity associated with metallic As^o precipitates in the insulating aluminum oxide matrix. With the assumption that this represents the entire increase and a Maxwell-Wagner form for the effective dielectric constant [7], the required volume fraction of elemental As would be approx. 6% for the high As content oxidized AlAs layer. The increase in bulk dielectric constant with increasing Ga content is likely due to increased bond polarizability associated with the Ga-O bonds. The dielectric constant of deposited Ga_2O_3 films has been reported to be up to 14.2 [8].

Table 1: Bulk Electrical Properties of Wet-Oxidized AlGaAs Films

Starting Composition	Arsenic	Leakage (A/cm^2 @ 5V)	Bulk Resistivity (Ohm-cm)	Bulk Dielectric Constant (1MHz)
AlAs	Low	$7.5x10^{-8}$	$2.7x10^{12}$	5.8
	High	$7.5x10^{-7}$	$2.7x10^{11}$	7.0
$Al_{0.98}Ga_{0.02}As$	Low	$2.9x10^{-9}$	$6.9x10^{13}$	6.2
	High	$2.5x10^{-7}$	$8.0x10^{11}$	8.3
$Al_{0.90}Ga_{0.10}As$	Low	$3.7x10^{-9}$	$5.4x10^{13}$	8.6
	High	$1.0x10^{-7}$	$1.2x10^{11}$	8.2

Capacitance-voltage (CV) measurements on thin oxidized $Al_xGa_{1-x}As$ layers (Fig.2) with residual As^0 at levels below the Raman detection limit (≈ 10-20-Å layers) [5] reveal partial Fermi-level pinning while measurements on layers with higher As^0 content exhibit strong Fermi-level pinning and no CV modulation. The presence of weak CV modulation and failure to reach the full accumulation capacitance in the low-As^0 samples would be consistent with the existence of an interface-state band located approximately 0.3 to 0.6 eV below the GaAs conduction band (CB) with a state density exceeding 10^{12} cm^{-2} and deep depletion at inversion biases. Given the ubiquitous presence of As^0 as detected near the interface by Raman in a large number of the samples, it is likely that local pinning of the Fermi-level at As^0 precipitates at the oxide/GaAs interface may be the source of the apparent high interface state density. The Schottky barrier height observed for the As^0/n-GaAs interface is 0.67 - 0.72 eV [9], which would appear as an apparent interface-state band below the level found here. However, if the As precipitates do not fully cover the oxide/GaAs interface, a situation may arise in which the Fermi-level at the interface may only be locally pinned and unpinned at other areas. The observed pinning positions of 0.3 to 0.6 eV below the GaAs CB may, therefore, alternatively be explained by non-uniform Fermi-level pinning at As crystallites at the interface (e.g., the formation of local barriers) with an areal coverage of As at the interface from about 83 - 98%. This non-uniform pinning of the Fermi-level at the oxide/GaAs interface would prevent the formation of a spatially uniform accumulation layer near the oxide interface and could explain the poor observed transconductance in field effect transistor (FET) devices employing oxidized $Al_xGa_{1-x}As$ gates.[2].

The continuing presence of residual As^0 at the oxide/GaAs interface even after lengthy oxidation is to be expected on thermodynamic considerations [10] when As_2O_3 is an oxidation

product, as we observe. Even if the As^0 formed from Al(Ga)As oxidation were totally removed, further generation of interfacial As^0 from oxidation of GaAs could proceed from the reaction

$$2\ GaAs + As_2O_3 = 4\ As + \beta\text{-}Ga_2O_3 \qquad \Delta G^0_f = -64\ kcal,\ \Delta H^0_f = -62\ kcal \qquad (1a).$$

Since interfacial As^0 even at the 10^{-4} monolayer level will degrade MIS performance, this poses a serious problem for achieving a viable GaAs MIS technology based on wet oxidation.

SUMMARY

Elemental As^0 and a-As_2O_3 form during AlGaAs wet oxidation. Their volatility is sufficient for them to serve as the primary species responsible for arsenic removal from the relatively porous oxidized film. Elemental As^0 is concentrated at the oxide /semiconductor interface in both crystalline and amorphous forms, with crystalline As^0 requiring longer reaction time for removal than amorphous As^0 when the oxidation front reaches the substrate GaAs. Thick (2-μm) Al-oxide films crystallize and delaminate after As^0 and a-As_2O_3 are removed by continued oxidation and/or heating, suggesting relatively weak adhesion that may be responsible for the fragility of some laterally oxidized optoelectronic structures. Both capacitance-voltage and dc transport behavior are degraded by the interfacial As^0. Non-uniform pinning of the Fermi-level at the oxide/GaAs interface by As precipitates may explain the strong Fermi-level pinning and have serious negative implications for FET devices. Good MIS devices will require As^0 removal without film crystallization. However, the fundamental limit imposed by the thermodynamically favored formation of elemental As at the interface makes this a formidable challenge.

ACKNOWLEDGEMENTS

This work was performed at Sandia National Laboratories and supported by the U.S. Department of Energy under Contract No. DE-AC04-94AL85000. Sandia is a multiprogram laboratory operated by Sandia Corporation , a Lockheed Martin Company, for the United States Department of Energy. The authors wish to thank Kent Geib and Denise Tibbetts-Russell for technical assistance.

REFERENCES

1. J.M. Dallesasse, N. Holonyak, Jr., A.R. Sugg, T.A. Richard, and N. El-Zein, Appl. Phys. Lett, **57**, 22844 (1990).
2. E.I.Chen, N.Holonyak, Jr., and S.A Maranowski, Appl. Phys. Lett. **66**, 2688, (1995).
3. ref to size effects of crystals paper: see implant damage etching paper for ref
4. G.P. Schwartz, B. Eschwartz, D. DiStefano, G.J. Gualtieri, and J.E. Griffiths, Appl. Phys. Lett. **34**, 205 (1979).
5. G.P. Schwartz, G.J. Gualtieri, J.E. Griffiths, C.D. Thurmond, B. Schwartz, J. Electrochem. Soc. **127**, 2488 (1980).
6. R.D. Twesten D.M. Follstaedt, K.D. Choquette, and R.P. Schneider, Jr. Appl. Phys. Lett. **69**, 19 (1996).
7. B. K. P. Scaife, Principles of Dielectrics (Clarendon Press, Oxford, 1989.)
8. M. Passlack, M. Hong, J. P. Mannaerts, Appl. Phys. Lett. **68**, 1099 (1996).
9. J.M. Woodall, P.D. Kirchner, J.F. Freeouf, D.T. McInturff, M.R. Melloch, F.H. Pollak, Phil. Trans. Roy. Soc. Lond. A **344**, 521 (1993).

10. C.D. Thurmond, G.P. Schwartz, G.W. Kammlott, and B. Schwartz, J. Electrochem Soc. **127**, 1366 (1980).

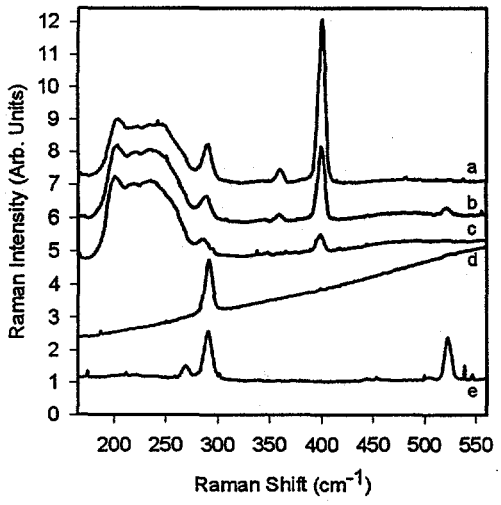

Fig. 1: Raman spectra of progressively oxidized 2.0-μm layer of $Al_{0.98}Ga_{0.02}As$ on GaAs: a-c) partially oxidized; d) oxidized "to completion"; e) layer crystallized and delaminating.

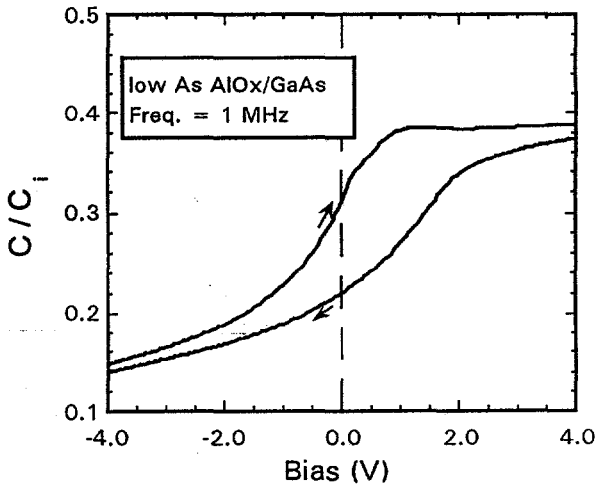

Fig. 2: Capacitance-voltage curve for MIS diode with 300-Å of oxidized AlAs on 2x10 ^{16} n-GaAs.

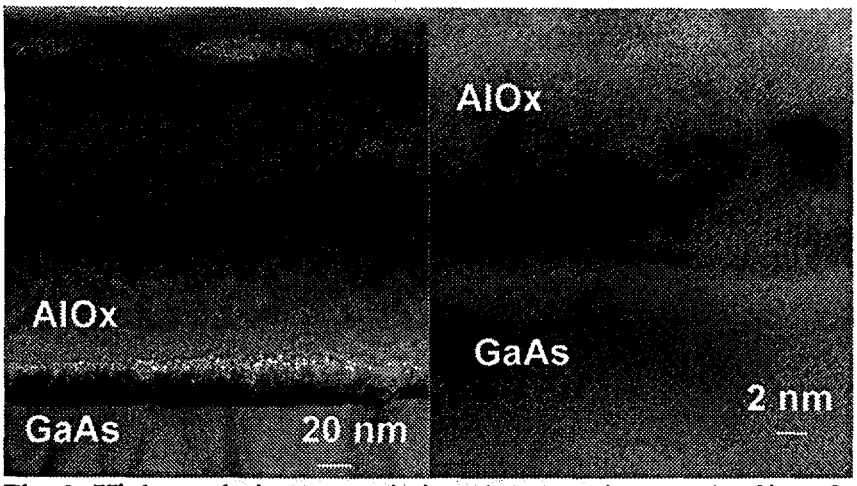

Fig. 3: High-resolution transmission electron micrograph of interfacial region of oxidized $Al_{0.90}Ga_{0.10}As$ as oxidation front approaches GaAs. Arsenic precipitates (2-4 nm) present at interface.